Characterization of YlxR/Ssr1238, a conserved RNA binding protein in a model cyanobacterium

Luisa Hemm[1], Anna Miucci[1], Matthias Riediger[1,#], Stefan Tholen[2], Jens Georg[1], Oliver Schilling[2] and Wolfgang R. Hess[1,*]

[1]Genetics and Experimental Bioinformatics, Faculty of Biology, Freiburg University, Germany;
[2]Institute for Surgical Pathology, Medical Center – University of Freiburg, Faculty of Medicine, University of Freiburg, Germany

[#]Current address: Capgemini, Berlin, Germany

*corresponding author: Wolfgang R. Hess: wolfgang.hess@biologie.uni-freiburg.de

Keywords: cyanobacteria, gene expression, photosynthesis, *Synechocystis* sp. PCC 6803, RNA binding proteins, RNase P

Abstract

Throughout the tree of life RNA-binding proteins play important roles in the regulation of gene expression and RNA metabolism, but they are only poorly characterized in cyanobacteria. Here, we analyzed the predicted RNA-binding protein Ssr1238 from the model cyanobacterium *Synechocystis* sp. PCC 6803. Ssr1238 is encoded in a syntenic region within the *nusA-ssr1238-infB* operon, similar to genes encoding such proteins in gram-positive bacteria. Overexpression of Ssr1238 for 24 h led to slightly higher levels of RNase P RNA, 44 tRNAs, and several stress-related mRNAs. Co-immunoprecipitation of proteins followed by MS analysis and sequencing of UV crosslinked, co-immunoprecipitated RNA samples identified potential interaction partners of Ssr1238. The most highly enriched transcript was RNase P RNA, and RnpA, the protein component of RNase P, was among the most highly enriched proteins, consistent with recent findings that YlxR proteins can influence the enzymatic activity of RNase P. A second highly enriched transcript derived from the 3' region of gene *ssl3177*, which encodes a rare lipoprotein homolog, a central enzyme in cell wall remodeling during cell division. The data also showed a strong connection to the RNA maturation and modification system indicated by co-precipitation of RNA methyltransferase Sll1967, the A-adding tRNA nucleotidyltransferase Sll1253, and queuine tRNA-ribosyltransferase Slr0713, as well as riboendonuclease E and enolase. Surprisingly, cyanophycin synthetase and urease were highly enriched as well. Therefore, Ssr1238 specifically binds to two different transcripts and appears to participate in the coordination of RNA maturation, aspects of nitrogen metabolism and translation, and cell division. Our results are consistent with recent findings that the *B. subtilis* YlxR protein functions as an RNase P modulator (RnpM), extend its proposed role to the phylum cyanobacteria, and suggest additional functionalities.

Introduction

RNA-binding proteins and cyanobacteria

RNA-binding proteins (RBPs) are crucial regulators of gene expression in all domains of life. Hundreds of previously unknown RBPs have recently been described from yeast to humans (1). In bacteria, RBPs accomplish functions as divergent as selectively protecting specific RNAs from degradation or recruiting the RNA degradosome to interact with a particular mRNA for degradation. Bacterial RBPs regulate the initiation of translation, terminate transcription (Rho) and are involved in matchmaking between an sRNA and its target mRNA (RNA chaperones such as Hfq or ProQ) or scaffolding (for a recent review, see (2)).

Cyanobacteria are the only bacteria whose physiology is based on oxygenic photosynthesis. Therefore, they are physiologically and genetically distant from gram-positive and gram-negative model bacteria such as *Bacillus subtilis* and *Escherichia coli*. A well-established model for cyanobacteria is the unicellular *Synechocystis* sp. PCC 6803 (*Synechocystis* 6803). *Synechocystis* 6803 was the first photosynthetic organism for which the total genome sequence was analyzed (3), and extensive datasets exist on the genome-wide regulation of gene expression (4) and active promoters (5), and on the suite of co-fractionating RNAs and proteins using gradient profiling by sequencing (Grad-seq) (6). Several sRNAs and riboswitches have been described in *Synechocystis* 6803, which regulate the responses to high light (7), low iron (8), or are involved in the control of mixotrophy (9), or nitrogen metabolism (10, 10, 11). However, no RNA chaperones or RBPs that mediate sRNA/mRNA duplex formation have been described in *Synechocystis* 6803 or any other cyanobacteria. Although a structural homolog of Hfq exists in most cyanobacteria, residues that are known to interact with RNA are not well conserved (12), and RNA-binding activity of Ssr3341, the Hfq homolog in *Synechocystis* 6803 (13), was not detected (14). Therefore, regulation by RBPs and their overall functions have not been well studied in cyanobacteria. One exception is a family of proteins containing the RNA-recognition motif (RRM), which exists in all cyanobacteria (15–20). For proteins belonging to this family, RNA binding was verified *in vitro* (21), and some RRM domain-containing RBPs (in *Synechocystis* 6803 Rbp2 and Rbp3) were found to be involved in the targeting of certain mRNAs to the thylakoid membrane system (22).

The Ssr1238/Slr0743a protein - an uncharacterized YlxR homolog

Ssr1238, also referred to as *slr0743a* in some genome annotations, is an 84 amino acids YlxR family protein that contains a DUF448 domain. Ssr1238 is a basic protein with a calculated isoelectric point of 11.09. In our previous work on *Synechocystis* 6803, it was predicted as a potential RBP based on Grad-seq results and a high support vector machine score for the prediction of RBPs from their amino acid sequences (6). Despite the shared presence of the YlxR domain, Ssr1238 is more distant to the YlxR proteins in *Bacillus subtilis* and *Streptococcus pneumoniae* or *Clostridioides difficile* with 24%, 24%, or 29% identical amino acids (**Figure 1**).

Initial evidence for YlxR proteins as RBPs was inferred from the structural analysis of the homolog in *S. pneumoniae* (23) and the in-gradient distribution of the *C. difficile* protein (24). The YlxR protein in *B. subtilis* has been described as a nucleoid-associated protein that regulates nearly 400 genes (25–27). Recently, the *Bacillus* YlxR protein has been reported to bind to the RNA subunit of the ribonuclease RNase P and modulate RNase P activity, leading to its renaming as an RNase P modulator (RnpM) (28). Compared to these YlxR homologs and to the structurally characterized *S. pneumonia* YlxR (23), several conserved residues previously discussed as possibly involved in RNA binding are widely conserved (R9, R19 and GRGA(W/Y) motif) in non-photosynthetic bacteria, as well as in cyanobacteria (**Figure 1**). However, residues K11, T15, V13, and D53, which have been shown to be critical for RNA binding in *Bacillus* RnpM, are not conserved in the *Synechocystis* protein Ssr1238. In addition, two pairs of cysteine residues present in the *C. difficile* YlxR homolog are conserved in Ssr1238 as well as in cyanobacterial homologs, but are partially lacking in RnpM and the homologs in other *Bacillus* and *Streptococcus* strains (**Figure 1**). Therefore, the function of cyanobacterial YlxR homologs as potential RBPs is not clear, nor is their possible regulatory role.

Cyanobacterial genomes are widely syntenic around the *ssr1238* locus. The *ssr1238* gene is located downstream of the *rimP* and *nusA* genes, encoding the ribosome maturation factor RimP, the transcription termination factor NusA and upstream of the *infB* gene, encoding the translation initiation factor InfB (arrangement *rimP-nusA-ssr1238-infB*) (6), thus suggesting a relationship to transcription and translation. Strikingly similar arrangements exist in Firmicutes and Actinobacteria indicating at the likely conservation of the underlying functionalities among these genes. The aim of this

study was to characterize the *Synechocystis* Ssr1238/YlxR protein by identifying possibly bound RNA molecules and interacting proteins.

Materials and Methods

Culturing conditions

Synechocystis 6803 PCC-M (29) wild type and mutant strains were cultivated in copper-free BG11 supplemented with 20 mM TES pH 7.5 under continuous white light of 50 µmol photons m^{-2} s^{-1} at 30°C. Mutant strains containing pVZ322-derived plasmids were cultivated in the presence of 2.5 µg/mL gentamycin.

Construction of mutant and tagged strains

The rhamnose-inducible promoter system (30, 31) was used to engineer strains that host the self-replicating pVZ322 plasmid (32) containing the *ssr1238-3×FLAG* or *sfGFP-3×FLAG* genes controlled by an inducible promoter . An intermediate cloning vector was prepared using the pUC19 plasmid as backbone. The sequence of the rhamnose construct starting at the *ilvBN* terminator and ending with the *rhaBAD* cassette of pCK355 (30) was amplified using Q5 polymerase (NEB), adding overlaps for AQUA cloning into pUC19 (33). The ECK120034435 terminator of pCK351 (30) was introduced downstream of the *yfp* gene to prevent readthrough. The sequence of the terminator was amplified using the Q5 polymerase adding overlaps for assembly into the cloned pUC19-P_{Rha}-YFP plasmid. The resulting plasmid was then subjected to inverse PCR to add the *ooP* terminator from *E. coli* downstream of the *rhaBAD* cassette and the 3×FLAG-tag downstream and in reading frame with the *yfp* gene. The corresponding PCR products were subjected to *Dpn*I digestion (Thermo Fisher Scientific), 5’ phosphorylation by T4 polynucleotide kinase (Thermo Fisher Scientific), self-ligation by T4 DNA ligase (Thermo Fisher Scientific) and heat shock transformation into chemically competent DH5α *E. coli* cells. The *yfp* gene was then replaced with either *ssr1238* or *sfgfp*. For this, the pUC19-P_{Rha}-YFP-3×FLAG plasmid was inverse amplified by PCR (Q5 polymerase, NEB), omitting the *yfp* gene. The *ssr1238* sequence was amplified from *Synechocystis* genomic DNA and the *sfgfp* sequence was amplified from plasmid pXG10-SF (34). Overlaps to the rhamnose promoter sequence and the 3×FLAG-tag were added to both sequences via the

respective primers. After assembly, plasmids pUC19-P_{Rha}-*ssr1238*-3×FLAG and pUC19-P_{Rha}-*sfGFP*-3×FLAG were obtained. The multi-host vector pVZ322 (32) was linearized using the restriction enzymes *Xba*I and *Xho*I (Thermo Fisher Scientific). Expression cassettes of *ssr1238* and *sfgfp* were amplified by PCR, adding overlaps to the linearized pVZ322. Throughout the cloning process, PCR products were subjected to a *Dpn*I digestion prior to the assembly to remove template DNA. Unless otherwise indicated, assembly was performed using the AQUA cloning protocol (33). Transformations were performed by heat shock into chemically competent *E. coli* DH5α cells. After each assembly and transformation step, colony PCRs (GOTAQ, NEB) were performed on positive *E. coli* clones to verify for correct transformation. PCR products for assembly were purified using the NucleoSpin Gel and PCR Clean-up Kit (Macherey-Nagel), and plasmids from positive clones were extracted using the NucleoSpin Plasmid Kit (Macherey-Nagel). Throughout the whole cloning process, intermediate and final plasmids were verified by Sanger sequencing (GATC, Eurofins). All primers are listed in **Supplementary Table S1** and the constructed plasmids in **Supplementary Table S2**.

Crosslinked immunoprecipitation and sequencing (CLIP-Seq)

Ssr1238-3×FLAG and sfGFP-3×FLAG expression was induced in 250 mL *Synechocystis* cultures with 0.6 mg/mL rhamnose at an OD_{750} of approximately 0.6-0.7. After 24 hours of induction, the cultures were transferred to a plastic tray measuring 21 cm x14.5 cm x 5.5 cm and crosslinked three times using a UV Stratalinker 2400 (Stratagene) at 0.45 J/cm^{-2}. Then, 25 mL culture aliquots were collected to prepare total RNA samples as controls for the corresponding samples and the comparison by RNA-seq. These aliquots were collected by vacuum filtration through hydrophilic polyethersulfone filters (Pall Supor®-800, 0.8 µm) and then snap frozen in liquid nitrogen. Next, 1 mL of PGTX (35) was added and RNA was extracted by incubating the samples at 65°C for 15 min. The samples were then washed and RNA precipitation was carried out as previously described (36). The remaining cultures were harvested via centrifugation at 4,000 x g for 20 min at 4°C. Afterwards, the cell pellets were resuspended in 1 mL of lysis buffer (20 mM Tris/HCl [pH 8.0], 1 mM $MgCl_2$, 150 mM KCl, 1 mM DTT) with 1 U of RNase inhibitor per sample (RiboLock, Thermo Fisher Scientific) to avoid RNA degradation during lysis. Cells were

mechanically disrupted using a pre-chilled Precellys 24 (Bertin Instruments) with 200 µL glass beads (Ø 0.1-0.25 mm, Retsch). Samples were spun at 3,000 x g for 2 min at 4°C to remove intact cells and glass beads. Any remaining cell debris was removed via centrifugation at 20,000 x g for 1h at 4°C. Purified lysates were coimmunoprecipitated by incubation with 50 µL packed bead volume of Anti-FLAG M2 magnetic beads (Sigma) for an hour at 4°C by slightly rotating. The DynaMag™-2 magnetic rack (Thermo Fisher Scientific) was used for flow-through removal and washing. Beads were washed twice with FLAG buffer, then twice with high salt FLAG buffer (50 mM HEPES/NaOH pH 7, 5 mM $MgCl_2$, 25 mM $CaCl_2$, 1 M NaCl, 10% glycerol, 0.1% Tween20), and then washed two more times with FLAG buffer. All washes used a 20x packed bead buffer volume and were performed at 4°C for 3 minutes. For subsequent Western blotting, 1/10 bead volumes were kept after the last washing step for immunodetection using the FLAG M2 monoclonal antiserum as described previously (37). Remaining beads were subjected to proteinase K digestion (1% SDS, 10 mM Tris-HCl pH 7.5, 100 µg/mL proteinase K) for 30 min at 50°C. Following that, 200 µL PGTX (35) was added and the samples were boiled for 15 min at 65°C to extract protein-bound RNA. After adding 140 µL chloroform/isoamyl alcohol (24:1), the samples were agitated and incubated for 10 min at room temperature. To obtain phase separation, the samples were centrifugated in a swing-out rotor at 3260 x g for 3 min at room temperature. The upper aqueous phase was transferred to an RNase-free tube and mixed in a 1:1 ratio with 100% EtOH. Mixtures were further cleaned using the clean and concentrator kit (Zymo Research). RNA was eluted in 15 µL RNase-free ddH2O. Construction of cDNA libraries and sequence analysis were performed by a commercial provider (Vertis Biotechnologie AG Freising, Germany). The RNA samples were fragmented using ultrasound (4 pulses of 30 sec each at 4°C). First, an oligonucleotide adapter was ligated to the 3' end of the RNA molecules. First-strand cDNA synthesis was performed using M-MLV reverse transcriptase and the 3’ adapter as primer. The first-strand cDNA was purified and the 5' Illumina TruSeq sequencing adapter was ligated to the 3' end of the antisense cDNA. The resulting cDNA was amplified by 13 cycles of PCR (15 to 18 for the negative control), to about 10-20 ng/µl using a high-fidelity DNA polymerase and introducing TruSeq barcode sequences as part of the 5' and 3' TruSeq sequencing adapters. The cDNA was purified using the Agencourt AMPure XP kit (Beckman Coulter Genomics) and analyzed by capillary electrophoresis. For Illumina NextSeq sequencing, the samples

were pooled in approximately equimolar amounts. The cDNA pool was size fractionated in the size range of 200 – 600 bp using a preparative agarose gel and sequenced on an Illumina NextSeq 500 system using 75 bp read length.

Raw reads of the RNA-sequencing were analyzed using the galaxy platform. The galaxy workflow can be accessed and reproduced at the following link: https://usegalaxy.eu/u/luisa_hemm/w/ylxr-3xflag-clip. In short, read quality was check with FastQC in the beginning. After the quality check, reads were mapped to the *Synechocystis* chromosome (GenBank accession NC_000911.1) and the 4 large plasmids pSYSA, pSYSG, pSYSM and pSYSX (NC_005230.1, NC_005231.1, NC_005229.1, NC_005232.1) using BWA-MEM (38) with default parameters. Resulting data were filtered using BAM filter (39) to remove unmapped reads as well as reads smaller than 20 nucleotides.

The annotation gff-file was based on the reference GenBank annotations amended by several additional genes based on transcriptomic analyses (5). htseq-count (40) (mode union, nonunique all, minaqual 0) was used to count the reads per transcript. Only transcripts with ≥ 10 reads in at least three samples were subjected to differential expression analysis with deseq2 (41). To visualize coverage of the reads, bam files were transformed into wiggle files using BAM to Wiggle (42). Wiggle single files were generated by summarizing the reads from the triplicate analyses for each position.

Protein co-immunoprecipitation and analyses by LC-MS/MS

Expression of Ssr1238-3×FLAG as well as sfGFP-3×FLAG was induced in 250 mL *Synechocystis* cultures at an OD_{750nm} of ~0.5 to 0.8 with 0.6 mg/mL rhamnose. Cells were collected by centrifugation at 4,000 × *g* and 4 °C for 20 min after 24 h of induction at an OD_{750nm} of ~0.6 to 0.9. The cell pellets were resuspended in approximately 1.5 mL of FLAG-MS buffer (50 mM HEPES/NaOH pH 7, 5 mM $MgCl_2$, 25 mM $CaCl_2$, 150 mM NaCl) containing protease inhibitor (c0mplete, Roche), mixed with 200 µL of glass beads (Ø 0.1-0.25 mm, Retsch) and lysed mechanically in a prechilled Precellys 24 (Bertin Instruments). To remove glass beads and intact cells, samples were centrifuged for 2 min at 3,000 × *g*. Supernatants were collected for further processing. To solubilize membrane proteins, the lysates were incubated for 45 min in the presence of 2 % n-dodecyl β-D-maltoside in the dark at 4°C. Afterwards, cell debris was removed by centrifugation (21,000 × *g*, 4°C, 1 h). Coimmunoprecipitation was performed by

incubating 75 µL packed volume of Anti-FLAG M2 magnetic beads (Sigma Aldrich) with the cleared lysate (1h, 4°C, rotating). Afterwards, the supernatant was removed using the DynaMag™-2 Magnet rack (Thermo Fisher Scientific) and the beads were washed 6 times with FLAG-MS buffer (20x packed bead volume).Western blots were performed as described previously (37) using 1/10 vol of beads and FLAG M2 monoclonal antiserum (Sigma) to verify protein pull down.

Remaining proteins were further processed according to the manufacturer's protocol for S-Trap micro filters (Protifi), using the provided buffers. Briefly, 23 µL of the 1x lysis buffer (5% SDS, 50 mM TEAB pH 8.5) was added to the beads and incubated at 95°C for 10 min to elute the proteins. Proteins were reduced by incubation with reduction buffer (end concentration 5 mM Tris(2-carboxyethyl)phosphine (TCEP)) for 15 min at 55°C and alkylated by incubation with alkylation buffer (end concentration 20 mM methyl methanethiosulfonate (MMTS)) for 10 min at room temperature in the dark. Afterwards, a final concentration of 1.2% phosphoric acid and then six volumes of binding buffer (90% methanol; 100 mM TEAB; pH 7.55) were added. After gentle mixing, the protein solution was loaded to an S-Trap filter and spun 3 times at 10,000 × *g* for 30 s. The filters were washed three times using 150 µL of binding buffer. Sequencing-grade trypsin (Promega, 1:25 enzyme:protein ratio) diluted in 20 µL digestion buffer (50 mM TEAB) were added to the filter and digested at 47 °C for 2 h. To elute peptides, three step-wise buffers were applied: a) 40 µL 50 mM TEAB, b) 40 µl 0.2% formic acid in H_2O, and c) 50% acetonitrile and 0.2% formic acid in H_2O. Each step was eluted by centrifugation (10,000 *x* g for 1 min). The peptide solutions were combined and dried in a SpeedVac (DNA 120, Savant).

Thereafter, the peptide concentration was measured using the BCA assay (Thermo Scientific). For LC-MS/MS measurements 800 ng of peptides were analyzed on a Q-Exactive Plus mass spectrometer (Thermo Scientific, San Jose, CA) coupled to an EASY-nLCTM 1000 UHPLC system (Thermo Scientific). The column setup consisted of an Acclaim™ PepMap™ 100 C18 column (Thermo Fisher Scientific, Cat. No. 164946) and a 200 cm µPac GEN1 analytical column (PharmaFluidics, 55250315018210) coupled to a Nanospray FlexTM ion source (Thermo Scientific, ES071) and a fused silica emitter (MS Wil, TIP1002005-5).

For peptide separation, a linear gradient of increasing buffer B (0.1% formic acid in 80% acetonitrile, Fluka) was applied, ranging from 5 to 50% buffer B over the first 80 min and from 50 to 100% buffer B in the subsequent 40 min (120 min separating

gradient length). Peptides were analyzed in data dependent acquisition mode (DDA). Survey scans were performed at 70,000 resolution, an AGC target of 3e6 and a maximum injection time of 50 ms followed by targeting the top 10 precursor ions for fragmentation scans at 17,500 resolution with 1.6 m/z isolation windows, an NCE of 30 and a dynamic exclusion time of 35 s. For all MS2 scans the intensity threshold was set to 1e5, the AGC to 1e4 and the maximum injection time to 80 ms.

Raw data were processed and analyzed with MaxQuant (Version 1.6.17.0) with the built-in Andromeda peptide search engine (43). The false discovery rate (FDR) at both the protein and peptide level was set to 1%. Two missed cleavage sites were allowed, no variable modifications were allowed, and carbamidomethylation of cysteines was set as fixed modification. The match between runs option was selected. For label free quantification the MaxLFQ algorithm was applied using the standard settings.
Only unique peptides were used for quantification. The database "Synechocystis sp. (strain PCC 6803 / Kazusa)" was downloaded from https://www.uniprot.org/proteomes/UP000001425 on Jun 9th, 2022. The proteome raw data acquired by MS were deposited at the ProteomeXchange Consortium (http://proteomecentral.proteomexchange.org) via the PRIDE partner repository (44) under the identifier PXD047746.
Data were normalized on peptide level by equalizing the medians using the MSstats package (v. 3.20.3) in R (v. 4.0.4) (45). Subsequently, protein LFQ intensities were $\log_2$ transformed. *P*-values were adjusted using the Benjamini-Hochberg procedure.
The intensities were compared using LFQ (label-free quantification) values (46) with Perseus (version 2.0.11 (47)). Contaminants, reverse sequences and proteins only identified by site were removed from the matrix and LFQ intensities were $\log_2$-transformed using Mstats (48). Before t-test and visualization using a volcano plot, the missing values were replaced by imputation with the normal distribution for each column separately (default settings). For hierarchical clustering (default parameters), only proteins with three valid values in at least one declared group (YlxR_3×FLAG and sGFP_3×FLAG) were considered.

Results

UV Crosslinking and sequencing provides evidence of YlxR/Ssr1238 interacting with two distinct transcripts

To determine potential RNA interaction partners of YlxR/Ssr1238, a pVZ322 plasmid was constructed in which a sequence encoding a triple FLAG epitope tag was fused to the 3' end of the *ssr1238* reading frame controlled by the P_{rha} promoter, which can be activated by the addition of rhamnose (49). Conjugation of this plasmid into *Synechocystis* 6803 yielded strain P_{rha}_*ssr1238*-3×FLAG. As control, a construct encoding a tagged superfolder green fluorescent protein (sfGFP) was engineered, yielding strain P_{rha}_*sfGFP*-3×FLAG.

The strains were cultivated in triplicate under identical conditions and crosslinked immunoprecipitation with subsequent sequencing (CLIP-Seq) was performed. After crosslinking with UV light, the Ssr1238 and sfGFP proteins were purified using magnetic beads binding to the FLAG epitope tag that was engineered at the C-terminal ends of the proteins. Purification of sfGFP and Ssr1238 was controlled by SDS-PAGE and western blotting, showing signals at the expected molecular masses of ~30 kDa (sfGFP_3×FLAG) and ~13 kDa (Ssr1238_3×FLAG; **Supplementary Figure S1**).

After protein purification, crosslinked RNA was extracted from the beads. As control for total transcript levels, total RNA of both strains was extracted in triplicate, yielding 12 samples in total. We obtained ~160 ± 60 ng of UV-clipped RNA from the Ssr1238_3×FLAG purification and 15 ± 4 ng of RNA for the sfGFP_3×FLAG negative control. For total RNA control samples, 4 to 24 µg of RNA was obtained. The ten-fold higher yield from the Ssr1238_3×FLAG purification compared to the sfGFP_3×FLAG sample indicated that RNA was bound by the former but less so by the latter. Comparison of the extracted RNA samples on a fragment analyzer revealed the enrichment of an RNA species of ~450 nt in the CLIP RNA of P_{rha}_*ssr1238*-3×FLAG, but not in the RNA extracted from the UV-treated P_{rha}_*sfGFP*-3×FLAG strain or in either of the unclipped controls (**Supplementary Figure S2**).

Next, cDNA libraries were prepared and sequenced on an Illumina NextSeq 500 system with 75 bp read length providing ~10,000,000 reads per sample.

The galaxy system (50) was used to analyze the sequencing data. The workflow is illustrated in **Supplementary Figure S3.**

To identify RNAs that specifically interacted with the Ssr1238_3×FLAG protein (XL-Ssr1238), the sequencing data were compared with the data obtained from cDNA analysis of RNA extracted from sfGFP_3×FLAG (XL-sfGFP). To obtain quantitative

data, log_2 fold changes (log_2 FC) were calculated and plotted over the adjusted *p*-values (**Figure 2A**). In the volcano plot, the transcript fragments with the highest log_2 FC compared to the sfGFP control are labelled. With the lowest *p*-value of 0.0 and a log_2FC of 5.969, RNase P RNA was the most-enriched transcript. The coverage pattern along the *rnpB* gene, from where RNase P RNA originates, showed contiguous coverage, with three distinct peaks (**Figure 2B**). In contrast, the coverage of *ssr1238* mRNA was almost identical in XL-Ssr1238 and in the cDNA analysis of total RNA with overexpressed *ssr1238* (OE-Ssr1238), and the coverage for both samples was much higher compared than that of the two sfGFP samples (XL-sfGFP and OE-sfGFP), consistent with its overexpression (**Figure 2C**). Therefore, *ssr1238* mRNA was not specifically enriched owing to crosslinking with YfrX/Ssr1238.

The list of all transcripts enriched in XL-Ssr1238 RNA compared to XL-sfGFP is given in **Supplementary Table S3** and the list of transcripts enriched in XL-Ssr1238 RNA compared to OE-Ssr1238 in **Supplementary Table S4**. In both comparisons we chose a minimum log_2 fold change (log_2FC) ≥1 and an adjusted *p*-value (padj) ≤0.05.

In addition to RNase P RNA, we noticed another particularly highly enriched transcript segment and several other slightly enriched peaks in the cDNA libraries generated from RNA crosslinked to YlxR/Ssr1238. The highly enriched transcript segment derived from the 3' region of gene *ssl3177* with a log_2FC +4.99 in the comparison XL-Ssr1238 / XL-sfGFP and a log_2FC of +4.01 in the comparison XL-Ssr1238 / OE-Ssr1238. The identified transcript segment interacting with YlxR/Ssr1238 was approximately 45 nt in length (**Figure 3A**). The segment contains a potentially strong helical structure of 37 nt (minimum free energy of -13.10 kcal/mol) and encompasses the last two codons and the *ssl3177* stop codon, together with the first 27 nt of the 3'UTR (**Figure 3B**). Therefore, it cannot constitute a classical 3' UTR-located Rho-independent terminator. Comparison of sequences from homologous loci in other *Synechocystis* strains revealed strong sequence and structure conservation (**Figure 3C**). These strains differ by several hundred genes from *Synechocystis* 6803 (51–53). Therefore, the conservation of the RNA fragment crosslinked to YlxR/Ssr1238 indicates its functional relevance.

However, annotation of *ssl3177* is conflicting. In most *Synechocystis* 6803 genome annotations it is a 90-codon reading frame encoding a protein with a truncated (partial) rare lipoprotein A domain. Resequencing the here employed laboratory substrain of *Synechocystis* 6803 revealed a single point mutation, G-->T, at position 1,012,958 in

the upstream region of *ssl3177* (29), indicating that this gene or upstream region is under evolutionary pressure. The gene *ssl3177* has remained uncharacterized experimentally thus far, but it has been found to be highly regulated in the context of carbon metabolism manipulation (54), iron starvation (55), osmotic stress (56), and in response to the depletion of the FtsH1/3 proteolytic complex (57), pointing to a central role of Ssl3177 in several different acclimation processes. Indeed, comparison of Ssl3177 to likely homologs (**Figure 3D**) revealed that the annotation of *ssl3177* should be corrected. The re-annotated coding sequence begins with an alternative TTG start codon (positions 1,012,946 to 1,012,948 on the reverse strand; GenBank accession NC_000911.1) and encodes the 110 amino acid rare lipoprotein A (gene *repA;* note that *Synechocystis* 6803 has a second rare lipoprotein A gene, called *rlpA, slr0423*), a central enzyme involved in cell wall remodeling during cell division (58). This function is also consistent with the genomic location of *repA*/*ssl3177* downstream of *ftsZ*. According to this reannotation and the fact that the transcription start site was mapped to position 1,012,976 (5), the 5 'UTR of *repA* is 28 nt and contains the previously reported point mutation at position 1,012,958 (29), only 10 nt upstream of the re-annotated start codon.

We conclude that YlxR/Ssr1238 binds to at least two distinct transcripts of *Synechocystis* 6803 *in vivo*. One of these transcripts is RNase P RNA and the other is an RNA fragment derived from the 3' end of the *ssl3177* gene encoding a rare lipoprotein A homolog.

Overexpression of YlxR/Ssr1238 leads to transcriptome changes

The 24 h induction period provided an opportunity for insight into possible consequences of increased YlxR/Ssr1238 expression. We calculated $\log_2$FC for the comparison of transcript levels between OE-Ssr1238 and OE-sfGFP (**Figure 4**). This comparison indicated that the transcript levels of 68 genes were upregulated and of another 57 genes were downregulated when requiring a $\log_2$FC ≥1 and a p_{adj} ≤0.05 (**Supplementary Table S5**).

Consistent with its intentional overexpression, *ssr1238* ($\log_2$FC of +3.446) was the most upregulated gene, followed by *sll1863*, *sll1862*, and *slr0093* encoding one of the seven DnaJ homologs, with $\log_2$FCs between +2.1 and 2.9. These genes have often been implicated in stress responses (59–61), and Sll1863, a protein of unknown

function, was previously identified as the most induced protein under salt stress (62). Along these lines, we also noticed an upregulation of *ggpR/ssl3076* (log_2FC of +1.872), the regulator mediating the salt-induced activation of glucosylglycerol synthesis in *Synechocystis* 6803 (63). To test for possible phenotypic effects, we spotted aliquots of cultures overexpressing *ssr1238* under 6 different conditions (**Supplementary Figure S4**). Although differences in growth were almost undetectable under standard growth conditions or with the addition of10 mM glucose, the overexpressing strains had a clear growth disadvantage under cold stress and at an elevated level of illumination.

Finally, *rnpB*, the gene from which the RNA component of RNase P is transcribed, was found upregulated (log_2FC of +1.512), indicating a possible stabilizing effect of YlxR/Ssr1238 overexpression. Intriguingly, the largest group of upregulated genes in the Ssr1238 overexpressor encompassed tRNA genes. In fact, we found that all 44 tRNA species present in *Synechocystis* 6803 were slightly more abundant in the OE-Ssr1238 strain, 16 of which had a significant log_2FC ≥1. One of these tRNA genes contains a group I intron in *Synechocystis* 6803 (**Supplementary Figure S5**). The intron is located within the gene for the initiator formylmethionine tRNA ($itRNA_{fmet}$). The complex gene arrangement in this genomic region is often misannotated, although this intron was first described 30 years ago (64). Relative to the tRNA structure, the intron is inserted within the anticodon loop. At the DNA level, the intron contains the protein-coding gene *slr0915* encoding the DNA double-strand homing endonuclease I-Ssp6803I (65). Furthermore, the $itRNA_{fmet}$ precursor transcript extends into the neighboring gene *slr0917* (*bioF*) encoding 8-amino-7-oxononanoate synthase. The entire segment, including the tRNA exons 1 and 2, the intron containing *slr0915,* and the downstream following gene *slr0917*, is transcribed from a single transcription start site 4 nt upstream of tRNA exon 1 into a single, contiguous transcription unit (TU) of 1,816 nt, classified as TU2935 in the genome-wide identification of transcription start sites (5) (**Supplementary Figure S5**). Here, we found log_2FCs for the different parts of this transcript as follows: tRNA-6803t34-gene ($itRNA_{fmet}$), +1.269; $itRNA_{fmet}$-intron-*bioF* precursor, +1.027 and *bioF* alone, +1.025. Moreover, we noticed a specific, slightly enriched, intron segment in the crosslinked RNA (see **Supplementary Figure S5**). This segment is located downstream of gene *slr0915* and comprises parts of intron domains P7, P8 and P9, including the pseudoknot formed between P8 and P3.

We conclude that 24 h of YlxR/Ssr1238 overexpression resulted in some, although not dramatic, changes in the transcriptome. The observed upregulation of both RNase P and tRNAs suggests at a possible stabilizing effect of YlxR/Ssr1238 upon binding, which likely contributes secondarily to the higher tRNA levels. In addition, *ssr1238* overexpression led to further changes in the composition of the transcriptome and affected vitality, which was more pronounced under certain stress conditions.

YlxR/Ssr1238 coimmunoprecipitates with proteins involved in RNA metabolism and nitrogen metabolism

To gain insight into the molecular mechanisms in which YlxR/Ssr1238 is involved, coimmunoprecipitation experiments were performed. A *Synechocystis* 6803 strain P_{rha}_*ssr1238*-3×FLAG was constructed to produce 3×FLAG-tagged YlxR/Ssr1238 from a plasmid pVZ322-located gene copy under the control of the rhamnose-inducible promoter P_{rha} (49). Twenty-four hours after induction, YlxR/Ssr1238-3×FLAG and bound interaction partners were immunoprecipitated from the lysate using anti-FLAG magnetic beads. In parallel, lysates from cultures expressing a tagged superfolder green fluorescent protein (sfGFP-3×FLAG) were purified. Both experiments were performed in triplicate.

Western blots were used for quality control of the protein pull-down for both proteins (**Supplementary Figure S6**). Signals of ~30 kDa in the crude extract, flow-through and elution fractions were obtained for the sfGFP-3×FLAG samples, while signals of ~13 kDa were obtained for the YlxR/Ssr1238-3×FLAG replicates. These signals were consistent with the expected molecular masses. Thus, the proteins were not lost during the preparation. The eluate fractions were analyzed by LC-MS/MS. A total of 1,010 proteins were detected in one or in both samples.

Statistical analysis indicated that a total of 234 proteins were enriched (152 significantly enriched) in the coimmunoprecipitation with YlxR/Ssr1238 compared to the sfGFP control (**Figure 5**). The complete list of detected proteins is shown in **Supplementary Table S6**.

Despite its small size of 84 amino acids, 4 unique peptides were detected for YlxR/Ssr1238. Furthermore, it was highly abundant according to LFQ values (**Supplementary Table S6)**, a measure corresponding to the sum of all the peptide intensities divided by the number of observable peptides of a protein (66). Among the

152 significantly enriched proteins, 24 were found exclusively in the YlxR/Ssr1238 coimmunoprecipitation and 190 were significantly enriched compared to their LFQ intensities in the sfGFP coimmunoprecipitation. The most enriched protein among the latter was YlxR/Ssr1238 with a log_2FC of 10.99.

Table 1 shows the 36 proteins that were enriched with a log_2FC ≥4 in the YlxR/Ssr1238 samples. Of these, several are related to RNA metabolism, RnpA, the protein component of ribonuclease P, the queuine tRNA-ribosyltransferase Slr0713, Sll1253, a 924 amino acids protein with a nanoRNase/pAp phosphatase domain and a separate A-adding tRNA nucleotidyltransferase domain, and finally enolase, an enzyme that is considered to be a component of the RNA degradosome (67).

A second functional category was formed by enriched proteins related to nitrogen metabolism. These proteins are cyanophycin synthetase (CphA) and all three urease subunits (UreA, UreB and UreC). CphA catalyzes the synthesis of the reserve polymer cyanophycin, an Asp-Arg polymer (68) and was the most enriched protein in the co-IP with YlxR/Ssr1238. Furthermore, the putative 8-amino-7-oxononanoate synthase BioF, encoded by *slr0917* in a co-transcript with the $itRNA_{fmet}$ (**Supplementary Figure S5**), was found. Finally, 3/36 highly enriched proteins perform completely unknown functions (**Table 1**).

Discussion

YlxR/Ssr1238 as an RNA-binding protein in *Synechocystis*

YlxR/Ssr1238 is the cyanobacterial homolog of the better studied YlxR protein in *Bacillus* (25, 26), recently renamed RpnM (28). However, the relatively low global sequence identity and deviations in certain amino acid positions critical for RNA binding (**Figure 1**) questioned the role of YlxR/Ssr1238 as an RBP. Therefore, we here performed UV crosslinking and sequencing of transcripts that were potentially bound to it. We found two highly enriched transcripts, RNase P RNA and the 3' segment of *repA*. The first result is consistent with findings for *Bacillus* (28) and indeed suggests a conserved function as a modulator of RNase P activity also in cyanobacteria. This interaction probably leads indirectly to the enrichment of RnpA, the protein component of RNase P, which is also bound to the RNase P RNA (**Figure 6**). Interestingly, we found some distinct differences in the transcriptomes of strains that were overexpressing YlxR/Ssr1238 or sfGFP as a control (**Figure 4**). These differences

included slightly elevated levels of tRNAs, caused by the likewise elevated RNase P RNA level. The overexpression of YlxR/Ssr1238 may be directly related to this effect by protecting the RNase P RNA from degradation. However, the broader physiological consequences of YlxR/Ssr1238 overexpression indicated the activation of several stress-related genes. Previous work in *Bacillus* revealed that the manipulation of YlxR expression affected the regulation of more than 400 genes and the response to glucose (25). Interestingly, there is a parallel in the work performed here, as YlxR/Ssr1238 overexpression led to opposite effects on two sRNA regulators that are involved in the regulation of mixotrophic versus photosynthetic lifestyles. While PsrR1, an sRNA regulator of several photosynthetic genes (7), showed an increased transcript level in OE-Ssr1238, the level of PmgR1, a regulator of mixotrophy (9), was decreased (**Figure 4, Supplementary Table S5**).

However, the second highly enriched transcript by UV crosslinking pointed in a different, very unexpected direction. The enriched *repA* 3' segment contains a strongly folded secondary structure that is not just a rho-independent terminator, but likely serves as a recognition domain for YlxR/Ssr1238. Moreover, this secondary structure is conserved among several homologs from other *Synechocystis* cyanobacteria (**Figure 3C**), ruling out the possibility that it is a randomly formed structure. The bound RNA segment contained the *repA* stop codon (**Figure 3B**). We therefore speculate that binding of YlxR/Ssr1238 to this region interferes with the completion of *repA* translation. Rare lipoproteins such as RepA are part of the divisome and elongasome complexes (69) and function as lytic transglycosylases, enzymes that are critical for cell wall remodeling during cell division (58). RlpA (in *Pseudomonas*) is present in higher amounts at the nascent septa of replicating bacteria while it is otherwise found at lower levels along the sidewall length of the bacterium (70). Therefore, the needed higher levels required for cell division may result from resumption of *repA* translation when YlxR binding is released, e.g. by switching to the RNase P RNA (**Figure 6**).

Proteins interacting with YlxR/Ssr1238

Finally, co-IP revealed a remarkable set of proteins that interact directly or indirectly with YlxR/Ssr1238. First, the enrichment of ribosomal proteins suggested a close association with ribosomes. An unexpected category of enriched proteins were four proteins related to nitrogen metabolism, all three urease subunits as well as

cyanophycin synthetase (CphA). Cyanophycin is a dynamic reserve polymer discovered 138 years ago (71). The relationship between CphA and YlxR/Ssr1238 is unknown, but a cycling of CphA between a granule-bound active and an inactive form in the cytosol has been described (72). It is therefore possible that YlxR/Ssr1238 is involved in the formation of the inactive form.

Furthermore, we noticed the enrichment of several enzymes related to RNA metabolism, such as the putative RNA methyltransferase Sll1967, the tRNA (guanine-N(7)-)-methyltransferase TrmB (Sll1300), the A-adding tRNA nucleotidyltransferase Sll1253, and the queuine tRNA ribosyltransferase Tgt (**Figure 5**). The co-enrichment of multiple enzymes involved in the RNA modification system is consistent with reports that the *Bacillus subtilis* YlxR regulates TsaD, a component of the TsaEBD system for the synthesis of the tRNA threonylcarbamoyl adenosine (t6A) modification (26). Consistent with strong interaction between YlxR/Ssr1238 and the RNAse P RNA was the co-enrichment of RnpA, i.e. the protein subunit of RNase P, in the co-IP experiments. Increasing numbers of adaptors or modulators of RNase activities are being identified in bacteria. Well-known examples are the RraA regulator of RNase E activity (73) and the *E. coli* RNase adaptor protein RapZ (74). Recently, an unrelated modulator of enzymatic activity has also been described for RNase E in cyanobacteria (75). According to the work of Wicke et al. (28) and based on the results of the present study, YlxR/Ssr1238 is another example of this category of regulatory proteins, but it primarily interacts with RNase P.

Another interesting co-enrichment was observed with RNase E (**Figure 5**), a central enzyme in the maturation and degradation of mRNAs in cyanobacteria (67). The co-enrichment of YlxR/Ssr1238 with RNase E is remarkable because RNase E is a central enzyme in mRNA maturation and degradation, while RNase P is best known for its crucial role in the maturation of tRNAs. However, there are several examples where both enzymes cooperate in the maturation of tRNA precursors in *E. coli* (76, 77), or in the generation of the 3' ends of three different proline tRNAs (78, 79). Recently, RNase E was also reported to be involved in the maturation of several tRNAs *in vivo* in *Synechocystis*, the most striking example being its involvement in in the accurate 5' maturation of the glutamyl-tRNA $tRNA^{Glu}_{UUC}$ (80). YlxR/Ssr1238 is a candidate protein to be physically involved in the crosstalk between both ribonucleases.

The results presented here are consistent with findings for the *Bacillus* YlxR homolog as an RNase P modulator (28), but extend its proposed role to the phylum

cyanobacteria and suggest a broader function in the integration of tRNA maturation, modification, protein synthesis, nitrogen metabolism and cell division.

Data availability

The CLIP-seq and RNA-seq data have been deposited in the SRA database under the BioProject accession number PRJNA1055971. Mass spectrometry raw data have been deposited at the ProteomeXchange Consortium (81) under the accession number PXD047746. Furthermore, all mass spectrometry proteomics datasets used and/or analyzed during this study are available online at the MassIVE repository (http://massive.ucsd.edu/; dataset identifier: MSV000093645.

Acknowledgments

We thank Janina Nandy for assistance in the construction of plasmids and Marcus Ziemann for help with the visualization of RNA read coverage.

Funding

Deutsche Forschungsgemeinschaft (DFG) via the graduate school MeInBio - 322977937/GRK2344 to L.H., O.S. and W.R.H. and by DFG grant HE 2544/22-1 to W.R.H. O.S. acknowledges support by DFG grant SCHI 871/11-1. The Proteomic Platform – Core Facility was supported by the Medical Faculty of the University of Freiburg to O.S. (2021/A3-Sch; 2023/A3-Sch). Supported by the Open Access Publication Fund of the University of Freiburg.

Conflict of interest

The authors declare that they have no conflict of interest.

Author Contributions

WRH and MR designed the project and WRH secured funding. ST and OS carried out MS-based proteomic analyses. JG contributed to the bioinformatic analyses. All other

experiments and analyses were performed by LH and AM. LH and WRH wrote the manuscript with input from all authors.

References

1. Hentze,M.W., Castello,A., Schwarzl,T. and Preiss,T. (2018) A brave new world of RNA-binding proteins. *Nat. Rev. Mol. Cell Biol.*, **19**, 327–341.
2. Ng Kwan Lim,E., Sasseville,C., Carrier,M.-C. and Massé,E. (2021) Keeping up with RNA-based regulation in bacteria: new roles for RNA binding proteins. *Trends Genet. TIG*, **37**, 86–97.
3. Kaneko,T., Sato,S., Kotani,H., Tanaka,A., Asamizu,E., Nakamura,Y., Miyajima,N., Hirosawa,M., Sugiura,M., Sasamoto,S., *et al.* (1996) Sequence analysis of the genome of the unicellular cyanobacterium *Synechocystis* sp. strain PCC6803. II. Sequence determination of the entire genome and assignment of potential protein-coding regions. *DNA Res.*, **3**, 109–136.
4. Hernández-Prieto,M.A., Semeniuk,T.A., Giner-Lamia,J. and Futschik,M.E. (2016) The transcriptional landscape of the photosynthetic model cyanobacterium *Synechocystis* sp. PCC6803. *Sci. Rep.*, **6**, 22168.
5. Kopf,M., Klähn,S., Scholz,I., Matthiessen,J.K.F., Hess,W.R. and Voß,B. (2014) Comparative analysis of the primary transcriptome of *Synechocystis* sp. PCC 6803. *DNA Res.*, **21**, 527–539.
6. Riediger,M., Spät,P., Bilger,R., Voigt,K., Macek,B. and Hess,W.R. (2021) Analysis of a photosynthetic cyanobacterium rich in internal membrane systems via gradient profiling by sequencing (Grad-seq). *Plant Cell*, **33**, 248–269.
7. Georg,J., Dienst,D., Schurgers,N., Wallner,T., Kopp,D., Stazic,D., Kuchmina,E., Klahn,S., Lokstein,H., Hess,W.R., *et al.* (2014) The small regulatory RNA SyR1/PsrR1 controls photosynthetic functions in cyanobacteria. *Plant Cell*, **26**, 3661–3679.
8. Georg,J., Kostova,G., Vuorijoki,L., Schön,V., Kadowaki,T., Huokko,T., Baumgartner,D., Müller,M., Klähn,S., Allahverdiyeva,Y., *et al.* (2017) Acclimation of oxygenic photosynthesis to iron starvation is controlled by the sRNA IsaR1. *Curr. Biol.*, **27**, 1425-1436.e7.
9. de Porcellinis,A.J., Klähn,S., Rosgaard,L., Kirsch,R., Gutekunst,K., Georg,J., Hess,W.R. and Sakuragi,Y. (2016) The non-coding RNA Ncr0700/PmgR1 is required for photomixotrophic growth and the regulation of glycogen accumulation in the cyanobacterium *Synechocystis* sp. PCC 6803. *Plant Cell Physiol.*, **57**, 2091–2103.
10. Klähn,S., Bolay,P., Wright,P.R., Atilho,R.M., Brewer,K.I., Hagemann,M., Breaker,R.R. and Hess,W.R. (2018) A glutamine riboswitch is a key element for the regulation of glutamine synthetase in cyanobacteria. *Nucleic Acids Res.*, **46**, 10082–10094.
11. Bolay,P., Hemm,L., Florencio,F.J., Hess,W.R., Muro-Pastor,M.I. and Klähn,S. (2022) The sRNA NsiR4 fine-tunes arginine synthesis in the cyanobacterium *Synechocystis* sp. PCC 6803 by post-transcriptional regulation of PirA. *RNA Biol.*, **19**, 811–818.
12. Bøggild,A., Overgaard,M., Valentin-Hansen,P. and Brodersen,D.E. (2009) Cyanobacteria contain a structural homologue of the Hfq protein with altered RNA-binding properties. *FEBS J.*, 10.1111/j.1742-4658.2009.07104.x.
13. Dienst,D., Dühring,U., Möllenkopf,H.-J., Vogel,J., Golecki,J., Hess,W.R. and Wilde,A. (2008) The cyanobacterial homologue of the RNA chaperone Hfq is essential for motility of *Synechocystis* sp. PCC 6803. *Microbiology*, **154**, 3134–3143.
14. Schuergers,N., Ruppert,U., Watanabe,S., Nürnberg,D.J., Lochnit,G., Dienst,D., Mullineaux,C.W. and Wilde,A. (2014) Binding of the RNA chaperone Hfq to the

type IV pilus base is crucial for its function in *S ynechocystis* sp. PCC 6803. *Mol. Microbiol.*, **92**, 840–852.
15. Dreyfuss,G., Swanson,M.S. and Piñol-Roma,S. (1988) Heterogeneous nuclear ribonucleoprotein particles and the pathway of mRNA formation. *Trends Biochem. Sci.*, **13**, 86–91.
16. Mulligan,M.E., Jackman,D.M. and Murphy,S.T. (1994) Heterocyst-forming filamentous cyanobacteria encode proteins that resemble eukaryotic RNA-binding proteins of the RNP family. *J. Mol. Biol.*, **235**, 1162–1170.
17. Sato,N. (1994) A cold-regulated cyanobacterial gene cluster encodes RNA-binding protein and ribosomal protein S21. *Plant Mol. Biol.*, **24**, 819–823.
18. Sugita,M. and Sugiura,M. (1994) The existence of eukaryotic ribonucleoprotein consensus sequence-type RNA-binding proteins in a prokaryote, Synechococcus 6301. *Nucleic Acids Res.*, **22**, 25–31.
19. Mulligan,M.E. and Belbin,T.J. (1995) Characterization of RNA-binding protein genes in cyanobacteria. *Nucleic Acids Symp. Ser.* **33**, 140-142.
20. Maris,C., Dominguez,C. and Allain,F.H.-T. (2005) The RNA recognition motif, a plastic RNA-binding platform to regulate post-transcriptional gene expression. *FEBS J.*, **272**, 2118–2131.
21. Sato,N. (1995) A family of cold-regulated RNA-binding protein genes in the cyanobacterium Anabaena variabilis M3. *Nucleic Acids Res.*, **23**, 2161–2167.
22. Mahbub,M., Hemm,L., Yang,Y., Kaur,R., Carmen,H., Engl,C., Huokko,T., Riediger,M., Watanabe,S., Liu,L.-N., *et al.* (2020) mRNA localization, reaction centre biogenesis and thylakoid membrane targeting in cyanobacteria. *Nat. Plants*, **6**, 1179–1191.
23. Osipiuk,J., Górnicki,P., Maj,L., Dementieva,I., Laskowski,R. and Joachimiak,A. (2001) Streptococcus pneumonia YlxR at 1.35 A shows a putative new fold. *Acta Crystallogr. D Biol. Crystallogr.*, **57**, 1747–1751.
24. Lamm-Schmidt,V., Fuchs,M., Sulzer,J., Gerovac,M., Hör,J., Dersch,P., Vogel,J. and Faber,F. (2021) Grad-seq identifies KhpB as a global RNA-binding protein in *Clostridioides difficile* that regulates toxin production. *microLife*, **2**, uqab004.
25. Ogura,M. and Kanesaki,Y. (2018) Newly identified nucleoid-associatedlLike protein YlxR regulates metabolic gene expression in *Bacillus subtilis*. *mSphere*, **3**, e00501-18.
26. Ogura,M., Sato,T. and Abe,K. (2019) *Bacillus subtilis* YlxR, which Is involved in glucose-responsive metabolic changes, regulates expression of *tsaD* for protein quality control of pyruvate dehydrogenase. *Front. Microbiol.*, **10**, 923.
27. Ogura,M., Shindo,K. and Kanesaki,Y. (2020) *Bacillus subtilis* nucleoid-associated protein YlxR is involved in bimodal expression of the fructoselysine utilization operon (*frlBONMD-yurJ*) promoter. *Front. Microbiol.*, **11**, 2024.
28. Wicke,D., Neumann,P., Gößringer,M., Chernev,A., Davydov,S., Poehlein,A., Daniel,R., Urlaub,H., Hartmann,R.K., Ficner,R., *et al.* (2023) The previously uncharacterized RnpM (YlxR) protein modulates the activity of ribonuclease P in *Bacillus subtilis* in vitro. *Nucleic Acids Res.*, 10.1093/nar/gkad1171.
29. Trautmann,D., Voß,B., Wilde,A., Al-Babili,S. and Hess,W.R. (2012) Microevolution in cyanobacteria: Re-sequencing a motile substrain of *Synechocystis* sp. PCC 6803. *DNA Res.*, **19**, 435–448.
30. Kelly,C.L., Taylor,G.M., Šatkutė,A., Dekker,L. and Heap,J.T. (2019) Transcriptional terminators allow leak-free chromosomal integration of genetic constructs in cyanobacteria. *Microorganisms*, **7**, 263.

31. Kelly,C.L., Taylor,G.M., Hitchcock,A., Torres-Méndez,A. and Heap,J.T. (2018) A rhamnose-inducible system for precise and temporal control of gene expression in cyanobacteria. *ACS Synth. Biol.*, **7**, 1056–1066.
32. Zinchenko,V.V., Piven,I.V., Melnik,V.A. and Shestakov,S.V. (1999) Vectors for the complementation analysis of cyanobacterial mutants. *Russ. J. Genet.*, **35**, 228–232.
33. Beyer,H.M., Gonschorek,P., Samodelov,S.L., Meier,M., Weber,W. and Zurbriggen,M.D. (2015) AQUA cloning: A versatile and simple enzyme-free cloning approach. *PLOS ONE*, **10**, e0137652.
34. Corcoran,C.P., Podkaminski,D., Papenfort,K., Urban,J.H., Hinton,J.C.D. and Vogel,J. (2012) Superfolder GFP reporters validate diverse new mRNA targets of the classic porin regulator, MicF RNA. *Mol. Microbiol.*, **84**, 428–445.
35. Pinto,F.L., Thapper,A., Sontheim,W. and Lindblad,P. (2009) Analysis of current and alternative phenol based RNA extraction methodologies for cyanobacteria. *BMC Mol. Biol.*, **10**, 79.
36. Hein,S., Scholz,I., Voß,B. and Hess,W.R. (2013) Adaptation and modification of three CRISPR loci in two closely related cyanobacteria. *RNA Biol.*, **10**, 852–864.
37. Baumgartner,D., Kopf,M., Klähn,S., Steglich,C. and Hess,W.R. (2016) Small proteins in cyanobacteria provide a paradigm for the functional analysis of the bacterial micro-proteome. *BMC Microbiol.*, **16**, 285.
38. Li,H. and Durbin,R. (2010) Fast and accurate long-read alignment with Burrows–Wheeler transform. *Bioinformatics*, **26**, 589–595.
39. Breese,M.R. and Liu,Y. (2013) NGSUtils: a software suite for analyzing and manipulating next-generation sequencing datasets. *Bioinforma. Oxf. Engl.*, **29**, 494–496.
40. Putri,G.H., Anders,S., Pyl,P.T., Pimanda,J.E. and Zanini,F. (2022) Analysing high-throughput sequencing data in Python with HTSeq 2.0. *Bioinformatics*, **38**, 2943–2945.
41. Love,M.I., Huber,W. and Anders,S. (2014) Moderated estimation of fold change and dispersion for RNA-seq data with DESeq2. *Genome Biol.*, **15**, 550.
42. Wang,L., Wang,S. and Li,W. (2012) RSeQC: quality control of RNA-seq experiments. *Bioinformatics*, **28**, 2184–2185.
43. Cox,J. and Mann,M. (2008) MaxQuant enables high peptide identification rates, individualized p.p.b.-range mass accuracies and proteome-wide protein quantification. *Nat. Biotechnol.*, **26**, 1367–1372.
44. Perez-Riverol,Y., Csordas,A., Bai,J., Bernal-Llinares,M., Hewapathirana,S., Kundu,D.J., Inuganti,A., Griss,J., Mayer,G., Eisenacher,M., *et al.* (2019) The PRIDE database and related tools and resources in 2019: improving support for quantification data. *Nucleic Acids Res.*, **47**, D442–D450.
45. Choi,M., Chang,C.-Y., Clough,T., Broudy,D., Killeen,T., MacLean,B. and Vitek,O. (2014) MSstats: an R package for statistical analysis of quantitative mass spectrometry-based proteomic experiments. *Bioinformatics*, **30**, 2524–2526.
46. Cox,J., Hein,M.Y., Luber,C.A., Paron,I., Nagaraj,N. and Mann,M. (2014) Accurate proteome-wide label-free quantification by delayed normalization and maximal peptide ratio extraction, termed MaxLFQ. *Mol. Cell. Proteomics*, **13**, 2513–2526.
47. Tyanova,S., Temu,T., Sinitcyn,P., Carlson,A., Hein,M.Y., Geiger,T., Mann,M. and Cox,J. (2016) The Perseus computational platform for comprehensive analysis of (prote)omics data. *Nat. Methods*, **13**, 731–740.
48. Kohler,D., Staniak,M., Tsai,T.-H., Huang,T., Shulman,N., Bernhardt,O.M., MacLean,B.X., Nesvizhskii,A.I., Reiter,L., Sabido,E., *et al.* (2023) MSstats

version 4.0: Statistical analyses of quantitative mass spectrometry-based proteomic experiments with chromatography-based quantification at scale. *J. Proteome Res.*, **22**, 1466–1482.

49. Kelly,C.L., Taylor,G.M., Hitchcock,A., Torres-Méndez,A. and Heap,J.T. (2018) A rhamnose-inducible system for precise and temporal control of gene expression in cyanobacteria. *ACS Synth. Biol.*, **7**, 1056–1066.
50. Afgan,E., Baker,D., Batut,B., van den Beek,M., Bouvier,D., Čech,M., Chilton,J., Clements,D., Coraor,N., Grüning,B.A., *et al.* (2018) The Galaxy platform for accessible, reproducible and collaborative biomedical analyses: 2018 update. *Nucleic Acids Res.*, **46**, W537–W544.
51. Kopf,M., Klähn,S., Voss,B., Stüber,K., Huettel,B., Reinhardt,R. and Hess,W.R. (2014) Finished genome sequence of the unicellular cyanobacterium *Synechocystis* sp. strain PCC 6714. *Genome Announc.*, **2**.
52. Kopf,M., Klähn,S., Pade,N., Weingärtner,C., Hagemann,M., Voß,B. and Hess,W.R. (2014) Comparative genome analysis of the closely related *Synechocystis* strains PCC 6714 and PCC 6803. *DNA Res.*, **21**, 255–266.
53. Jeong,Y., Hong,S.-J., Cho,S.-H., Yoon,S., Lee,H., Choi,H.-K., Kim,D.-M., Lee,C.-G., Cho,S. and Cho,B.-K. (2021) Multi-omic analyses reveal habitat adaptation of marine cyanobacterium *Synechocystis* sp. PCC 7338. *Front. Microbiol.*, **12**, 667450.
54. Orf,I., Klähn,S., Schwarz,D., Frank,M., Hess,W.R., Hagemann,M. and Kopka,J. (2015) Integrated analysis of engineered carbon limitation in a quadruple CO2/HCO3− uptake mutant of *Synechocystis* sp. PCC 6803. *Plant Physiol.*, **169**, 1787–1806.
55. Hernández-Prieto,M.A., Schön,V., Georg,J., Barreira,L., Varela,J., Hess,W.R. and Futschik,M.E. (2012) Iron deprivation in *Synechocystis*: Inference of pathways, non-coding RNAs, and regulatory elements from comprehensive expression profiling. *G3 Genes Genomes Genetics*, **2**, 1475–1495.
56. Mikami,K., Kanesaki,Y., Suzuki,I. and Murata,N. (2002) The histidine kinase Hik33 perceives osmotic stress and cold stress in *Synechocystis* sp. PCC 6803. *Mol. Microbiol.*, **46**, 905–915.
57. Krynická,V., Georg,J., Jackson,P.J., Dickman,M.J., Hunter,C.N., Futschik,M.E., Hess,W.R. and Komenda,J. (2019) Depletion of the FtsH1/3 proteolytic complex suppresses the nutrient stress response in the cyanobacterium *Synechocystis* sp strain PCC 6803. *Plant Cell*, **31**, 2912–2928.
58. Jorgenson,M.A., Chen,Y., Yahashiri,A., Popham,D.L. and Weiss,D.S. (2014) The bacterial septal ring protein RlpA is a lytic transglycosylase that contributes to rod shape and daughter cell separation in *Pseudomonas aeruginosa*. *Mol. Microbiol.*, **93**, 113–128.
59. Hihara,Y., Sonoike,K., Kanehisa,M. and Ikeuchi,M. (2003) DNA microarray analysis of redox-responsive genes in the genome of the cyanobacterium *Synechocystis* sp. strain PCC 6803. *J. Bacteriol.*, **185**, 1719–1725.
60. Georg,J., Rosana,A.R.R., Chamot,D., Migur,A., Hess,W.R. and Owttrim,G.W. (2019) Inactivation of the RNA helicase CrhR impacts a specific subset of the transcriptome in the cyanobacterium *Synechocystis* sp. PCC 6803. *RNA Biol.*, **16**, 1205–1214.
61. Klähn,S., Mikkat,S., Riediger,M., Georg,J., Hess,W.R. and Hagemann,M. (2021) Integrative analysis of the salt stress response in cyanobacteria. *Biol. Direct*, **16**, 26.

62. Fulda,S., Mikkat,S., Schröder,W. and Hagemann,M. (1999) Isolation of salt-induced periplasmic proteins from *Synechocystis* sp. strain PCC 6803. *Arch. Microbiol.*, **171**, 214–217.
63. Klähn,S., Höhne,A., Simon,E. and Hagemann,M. (2010) The gene *ssl3076* encodes a protein mediating the salt-induced expression of *ggpS* for the biosynthesis of the compatible solute glucosylglycerol in *Synechocystis* sp. strain PCC 6803. *J. Bacteriol.*, **192**, 4403–4412.
64. Biniszkiewicz,D., Cesnaviciene,E. and Shub,D.A. (1994) Self-splicing group I intron in cyanobacterial initiator methionine tRNA: evidence for lateral transfer of introns in bacteria. *EMBO J.*, **13**, 4629–4635.
65. Bonocora,R.P. and Shub,D.A. (2001) A novel group I intron-encoded endonuclease specific for the anticodon region of tRNA(fMet) genes. *Mol. Microbiol.*, **39**, 1299–1306.
66. Schwanhäusser,B., Busse,D., Li,N., Dittmar,G., Schuchhardt,J., Wolf,J., Chen,W. and Selbach,M. (2011) Global quantification of mammalian gene expression control. *Nature*, **473**, 337–342.
67. Zhang,J.-Y., Hess,W.R. and Zhang,C.-C. (2022) “Life is short, and art is long”: RNA degradation in cyanobacteria and model bacteria. *mLife*, **1**, 21–39.
68. Aboulmagd,E., Oppermann-Sanio,F.B. and Steinbüchel,A. (2000) Molecular characterization of the cyanophycin synthetase from *Synechocystis* sp. strain PCC6308. *Arch. Microbiol.*, **174**, 297–306.
69. Avila-Cobian,L.F., De Benedetti,S., Kim,C., Feltzer,R., Champion,M.M., Fisher,J.F. and Mobashery,S. (2022) In vitro studies of the protein-interaction network of cell-wall lytic transglycosylase RlpA of *Pseudomonas aeruginosa*. *Commun. Biol.*, **5**, 1314.
70. Avila-Cobian,L.F., Hoshino,H., Horsman,M.E., Nguyen,V.T., Qian,Y., Feltzer,R., Kim,C., Hu,D.D., Champion,M.M., Fisher,J.F., *et al.* (2023) Amber-codon suppression for spatial localization and in vivo photoaffinity capture of the interactome of the *Pseudomonas aeruginosa* rare lipoprotein A lytic transglycosylase. *Protein Sci.*, **32**, e4781.
71. Borzi,A. (1886) Le comunicazioni intracellulari delle Nostochinee. *Malpighia*, **1**, 28–74.
72. Watzer,B. and Forchhammer,K. (2018) Cyanophycin synthesis optimizes nitrogen utilization in the unicellular cyanobacterium *Synechocystis* sp. strain PCC 6803. *Appl. Environ. Microbiol.*, **84**, e01298-18.
73. Górna,M.W., Pietras,Z., Tsai,Y.-C., Callaghan,A.J., Hernández,H., Robinson,C.V. and Luisi,B.F. (2010) The regulatory protein RraA modulates RNA-binding and helicase activities of the *E. coli* RNA degradosome. *RNA*, **16**, 553–562.
74. Göpel,Y., Papenfort,K., Reichenbach,B., Vogel,J. and Görke,B. (2013) Targeted decay of a regulatory small RNA by an adaptor protein for RNase E and counteraction by an anti-adaptor RNA. *Genes Dev.*, **27**, 552–564.
75. Liu,S.-J., Lin,G.-M., Yuan,Y.-Q., Chen,W., Zhang,J.-Y. and Zhang,C.-C. (2023) A conserved protein inhibitor brings under check the activity of RNase E in cyanobacteria. *Nucleic Acids Res.*, 10.1093/nar/gkad1094.
76. Li,Z. and Deutscher,M.P. (2002) RNase E plays an essential role in the maturation of *Escherichia coli* tRNA precursors. *RNA*, **8**, 97–109.
77. Mohanty,B.K. and Kushner,S.R. (2022) Processing of the *alaW alaX* operon encoding the Ala2 tRNAs in *Escherichia coli* requires both RNase E and RNase P. *Mol. Microbiol.*, **118**, 698–715.

78. Mohanty,B.K., Petree,J.R. and Kushner,S.R. (2016) Endonucleolytic cleavages by RNase E generate the mature 3′ termini of the three proline tRNAs in *Escherichia coli*. *Nucleic Acids Res.*, **44**, 6350–6362.
79. Mohanty,B.K., Maples,V. and Kushner,S.R. (2022) The C nucleotide at the mature 5' end of the *Escherichia coli* proline tRNAs is required for the RNase E cleavage specificity at the 3' terminus as well as functionality. *Nucleic Acids Res.*, **50**, 1639–1649.
80. Hoffmann,U.A., Lichtenberg,E., Rogh,S.N., Bilger,R., Reimann,V., Heyl,F., Backofen,R., Steglich,C., Hess,W.R. and Wilde,A. (2023) The role of the 5' sensing function of ribonuclease E in cyanobacteria. *bioRxiv*, 10.1101/2023.01.13.523895.
81. Deutsch,E.W., Bandeira,N., Perez-Riverol,Y., Sharma,V., Carver,J.J., Mendoza,L., Kundu,D.J., Wang,S., Bandla,C., Kamatchinathan,S., *et al.* (2023) The ProteomeXchange consortium at 10 years: 2023 update. *Nucleic Acids Res.*, **51**, D1539–D1548.
82. Gruber,A.R., Bernhart,S.H. and Lorenz,R. (2015) The ViennaRNA web services. *Methods Mol. Biol. Clifton NJ*, **1269**, 307–326.
83. Will,S., Joshi,T., Hofacker,I.L., Stadler,P.F. and Backofen,R. (2012) LocARNA-P: accurate boundary prediction and improved detection of structural RNAs. *RNA,* **18**, 900–914.
84. Larkin,M.A., Blackshields,G., Brown,N.P., Chenna,R., McGettigan,P.A., McWilliam,H., Valentin,F., Wallace,I.M., Wilm,A., Lopez,R., *et al.* (2007) Clustal W and Clustal X version 2.0. *Bioinformatics*, **23**, 2947–2948.
85. Albà,M. (2000) Making alignments prettier. *Genome Biol.*, **1**, reports2047.
86. Tusher,V.G., Tibshirani,R. and Chu,G. (2001) Significance analysis of microarrays applied to the ionizing radiation response. *Proc. Natl. Acad. Sci.*, **98**, 5116–5121.

Tables

Table 1. Most enriched proteins identified by MS analysis for FLAG affinity co-immunoprecipitation of samples containing 3×FLAG-tagged Ssr1238/YlxR versus 3×FLAG-tagged sfGFP (log_2FC ≥4). Given is the gene name followed by the locus ID, the uniport ID, the log_2FC value and the function. Boldface letters indicate proteins related to RNA metabolism. Acronyms: MW, molecular weight in kDa; PSII, photosystem II. The experiment was performed in biological triplicate.

Gene	Locus ID	Protein ID	log_2FC	MW	Function
cphA	slr2002	P73833	13.53	94.69	cyanophycin synthetase
ylxR	**ssr1238**	**A0A8F1D7B1**	**11.31**	**9.73**	**modulator of RNase P activity RnpM**
ureC	sll1750	P73061	8.20	61.04	urease alpha subunit
slr0930	slr0930	Q55502	8.01	49.36	DUF815 domain / P-loop containing nucleotide triphosphate hydrolase protein
ureB	sll0420	P74386	7.36	11.38	urease beta subunit
pyrH	**sll0144**	**P74457**	**7.18**	**27.65**	**uridylate kinase**
ureA	slr1256	P73796	6.82	11.06	urease gamma subunit
rnpA	**slr1469**	**Q55005**	**6.76**	**14.50**	**ribonuclease P subunit A**
pmbA	slr1435	P73501	6.25	46.38	PmbA/TldA metallopeptidase
sll1456	sll1456	P73445	6.20	33.52	SAM-dependent methyltransferase
slr1470	slr1470	P74154	6.18	14.90	PSII auxillary membran protein
slr0863	slr0863	P73754	6.14	50.37	metalloprotease
lexA	sll1626	P73722	5.97	22.74	transcription regulator
slr1363	slr1363	P73537	5.86	58.90	polyphosphate kinase-2-related protein
fpg	slr1689	P74290	5.84	32.06	formamidopyrimidine-DNA glycosylase MutM
tgt	**slr0713**	**Q55983**	**5.80**	**41.50**	**queuine tRNA-ribosyltransferase**
bvdR	slr1784	P72782	5.79	36.64	biliverdin reductase
hisZ	slr1560	P74592	5.73	44.28	ATP phosphoribosyltransferase regulatory subunit
ppc	sll0920	P74299	5.45	118.94	phosphoenolpyruvate carboxylase
eno	**slr0752**	**P77972**	**5.16**	**46.53**	**enolase, degradosome**
slr1503	slr1503	P73939	5.05	36.51	NADP-dependent oxidoreductase
sll0400	sll0400	Q55129	5.00	18.27	phosphatase
slr0600	slr0600	P74746	4.96	35.99	NADPH-thioredoxin reductase
prsA	**sll0469**	**Q55848**	**4.78**	**36.40**	**ribose-phosphate pyrophosphokinase**
sll0294	sll0294	Q55546	4.77	45.57	unknown
lpxA	sll0379	Q55746	4.73	30.00	acyl-[acyl-carrier-protein]--UDP-N-acetylglu-cosamine O-acyltransferase
flv2	sll0219	P72721	4.60	65.60	flavodiiron protein Flv2
slr1218	slr1218	P73461	4.36	17.68	unknown
sigC	sll0184	Q59996	4.34	46.58	RNA polymerase sigma-C factor
rpoC2	sll1789	P73334	4.18	144.78	RNA polymerase subunit beta'
pcnB	**sll1253**	**P74081**	**4.14**	**105.91**	**A-adding tRNA nucleotidyltransferase / nanoRNase/pAp phosphatase domain**

sll2008	sll2008	P73670	4.13	47.98	processing protease
bioF	slr0917	P74770	4.11	42.92	8-amino-7-oxononanoate synthase
hisG	sll0900	Q55503	4.09	23.44	ATP phosphoribosyltransferase
sll1318	sll1318	P72733	4.09	24.95	unknown
aroQ	sll1112	P73367	4.01	16.37	3-dehydroquinate dehydratase

Figures

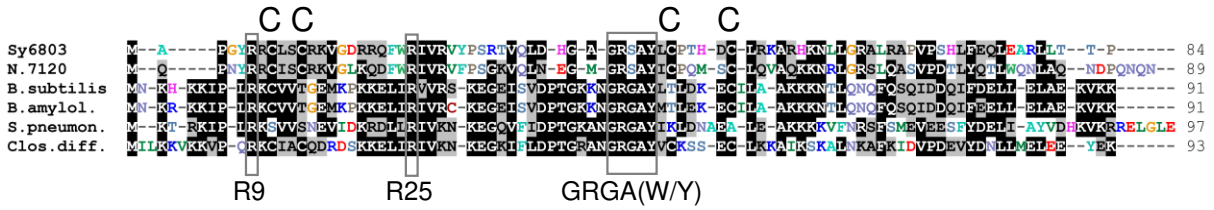

Figure 1. Multiple sequence alignment of YlxR homologs from different species. The homologs are from the two cyanobacteria *Synechocystis* (Sy6803; Ssr1238) and *Nostoc* sp. PCC 7120 (N.7120; Asr2830), compared to sequences from *Bacillus subtilis* subsp. subtilis str. 168 (B.subtilis; NP_389543), *Bacillus amyloliquefaciens* (B.amylol.; WP_158185884), *Streptococcus pneumoniae* (S.pneumon.; BEL22271) and *Clostridioides difficile* (Clos.diff.; CEJ97888). Identical and at least 50% conserved residues are shaded black. The residues R9, R25 and the GRGA(W/Y) motif are indicated which in the *Streptococcus pneumonia* homolog were discussed as involved in RNA binding (23). Capital Cs on top of the alignment indicate two pairs of cysteine residues shared between Ssr1238 and homologs in other cyanobacteria and in *C. difficile*.

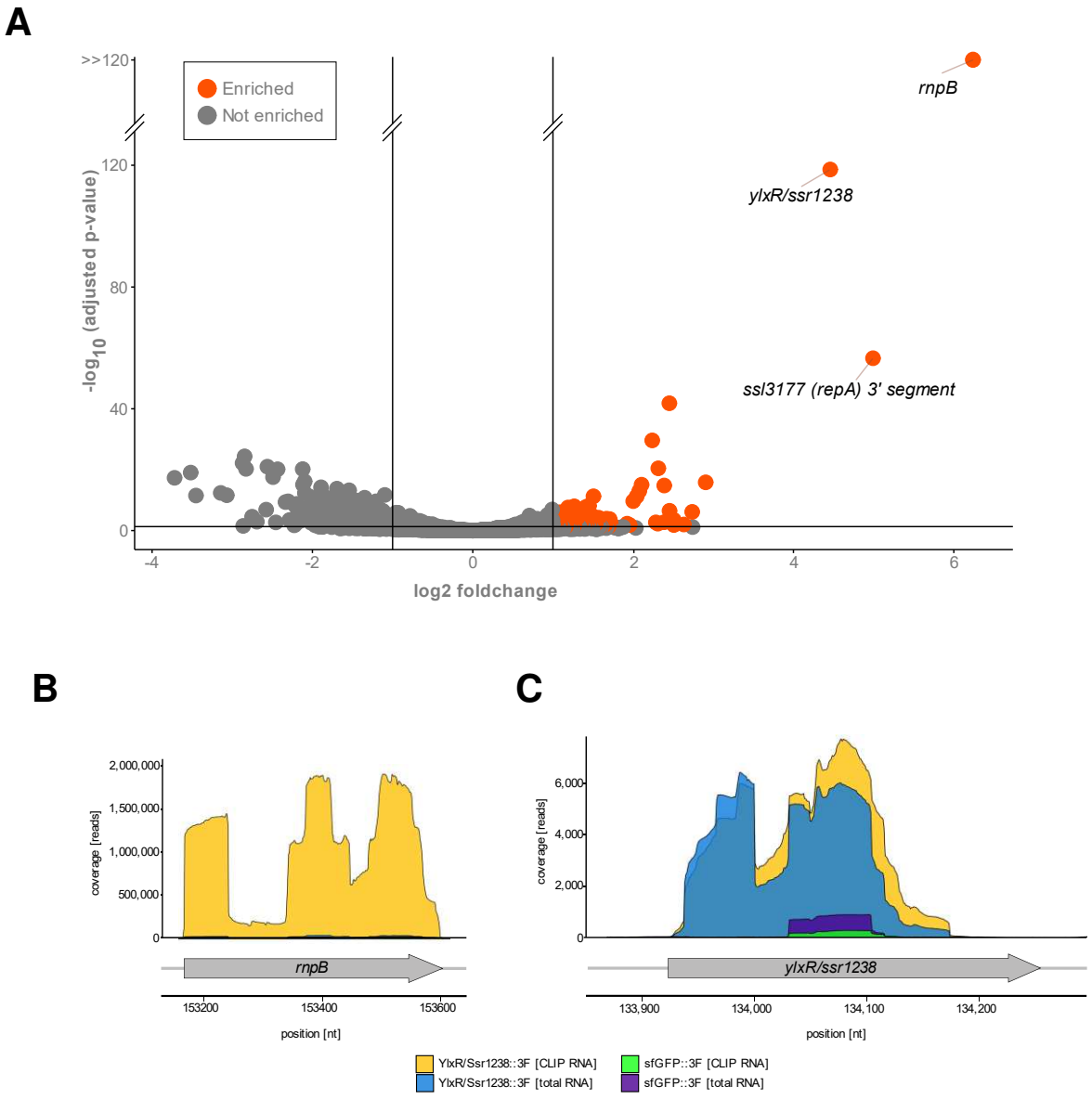

Figure 2. Transcripts enriched with YlxR/Ssr1238 after UV crosslinking in *Synechocystis*. A. Volcano plot showing transcripts enriched in the Ssr1238_3×FLAG CLIP RNA samples compared to the sfGFP_3×FLAG CLIP RNA samples (n=3). The -$\log_{10}$ adjusted *p*-values are plotted against the $\log_2$ fold changes. Red dots indicate enriched transcripts and gray dots indicate non-enriched transcripts. Gene IDs are given for the three most enriched transcripts (*rnpB*, RNase P RNA; *ylxR/ssr1238*, mRNA of the overexpressed gene; *ssl3177 (repA*), 3' segment of coding sequence and 3' UTR, see **Figure 3** for details). The full list is provided in **Supplementary Table S3**. **B.** Read coverage for the 4 different samples at the *rnpB* locus. **C.** Read coverage at the *ylxR/ssr1238* gene. Read coverages are given along the y-axis, genomic positions (GenBank accession NC_000911.1) along the x-axis. The different samples compared

are color-coded as indicated in the legend (CLIP RNA, crosslinked RNA; total RNA, RNA-seq data from cultures overexpressing *ylxR/ssr1238* or *sfGFP*), n=3.

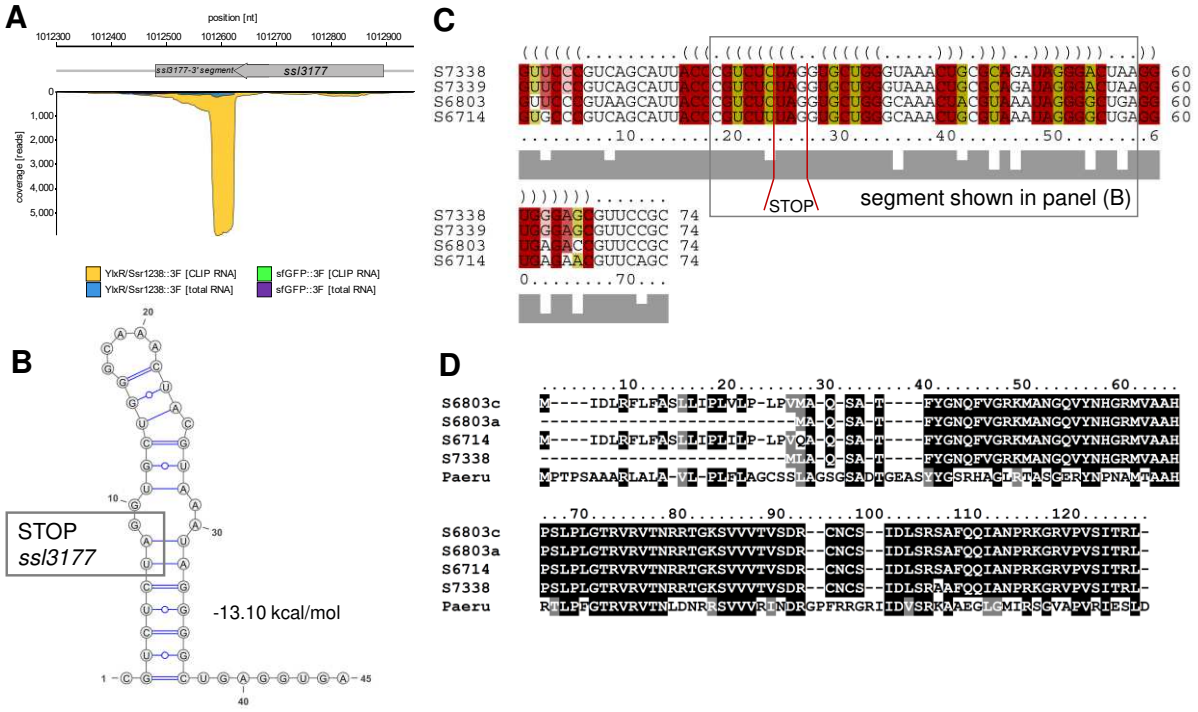

Figure 3. Interaction of YlxR/Ssr1238 with an *ssl3177* mRNA 3' end-derived transcript segment. A. Crosslinked transcript segment (grey, XL YlxR/Ssr1438, all colors as in **Figure 2B** and **C**). **B.** A stem-loop secondary structure within the enriched transcript segment as predicted by RNAfold (82) accessed at http://rna.tbi.univie.ac.at//cgi-bin/RNAWebSuite/RNAfold.cgi. The *ssl3177* stop codon and the calculated minimum folding energy are indicated. **C.** LocaRNA (83) alignment of the segment shown in panel (B) including some up- and downstream positions with homologous sequences from *Synechocystis* spp. PCC 6714, PCC 7338 and PCC 7339. The segment from panel (B) is boxed and the stop codon indicated. The webserver at https://rna.informatik.uni-freiburg.de/LocARNA/Input.jsp was used. **D.** Comparison of the annotated *ssl3177* in *Synechocystis* 6803 (S6803a), as corrected based on the considerations in this study (S6803c), and in strains *Synechocystis* PCC 6714 and PCC 7338/7339 and the functionally characterized homolog from *Pseudomonas aeruginosa* (58). The alignment was obtained using Clustal X (84) as implemented in Bioedit v7.2.6 and shaded using Boxshade (85) v3.3 accessed at https://junli.netlify.app/apps/boxshade/.

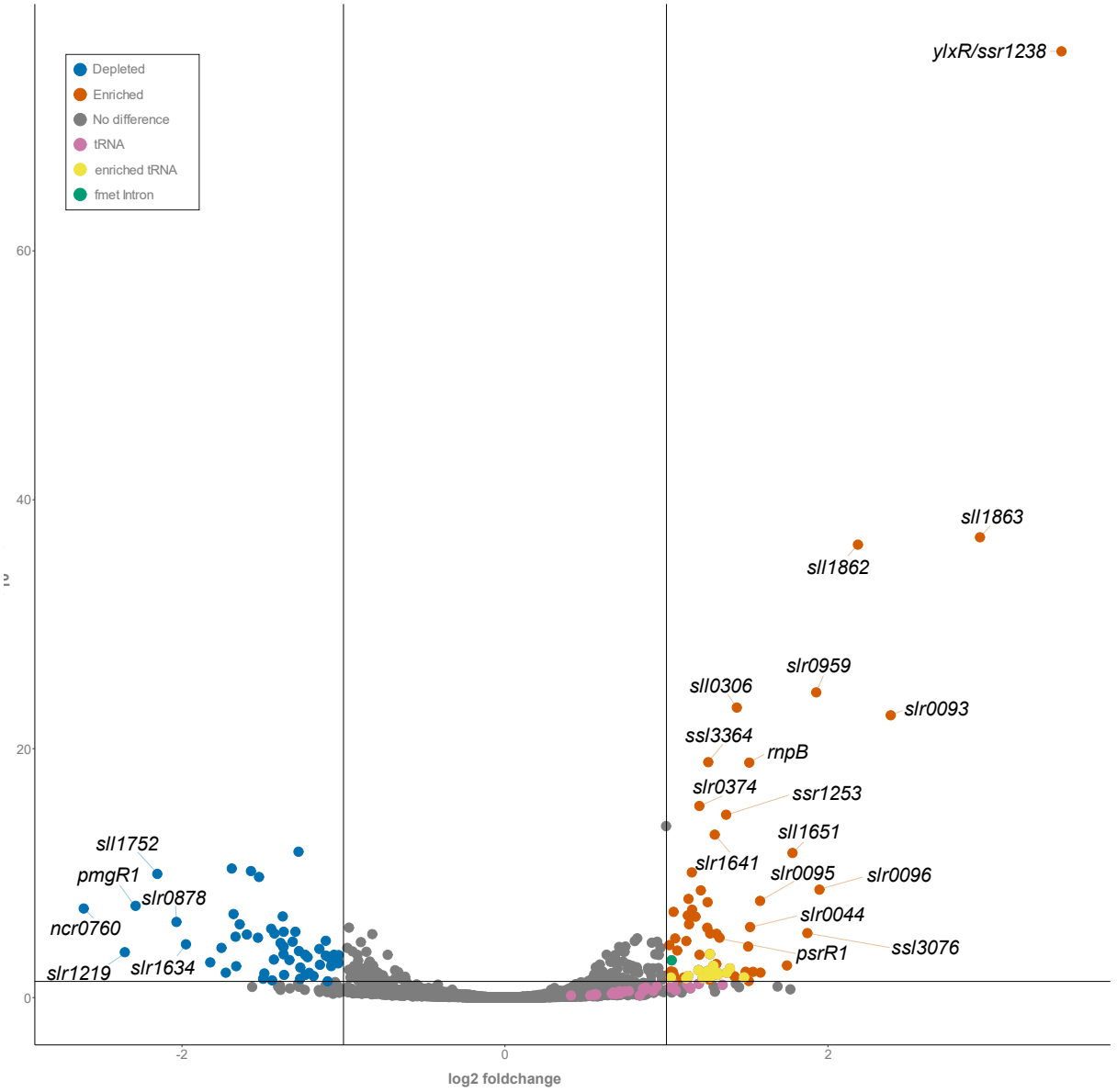

Figure 4. RNA-seq analysis of up- and down-regulated genes upon overexpression of YlxR/Ssr1238. Volcano plot showing transcripts upregulated in OE-Ssr1238 compared to OE-sfGFP. The red dots indicate upregulated mRNAs and non-coding RNAs (*rnpB*, RNase P RNA; *psrR1*, photosynthesis regulatory RNA 1), yellow and magenta dots indicate upregulated tRNAs and a green dot the itRNA$_{fmet}$ intron fragment. Blue dots indicate down-regulated transcripts (*pmgR1*, photomixotrophic growth RNA 1). See **Supplementary Table S5** for full details.

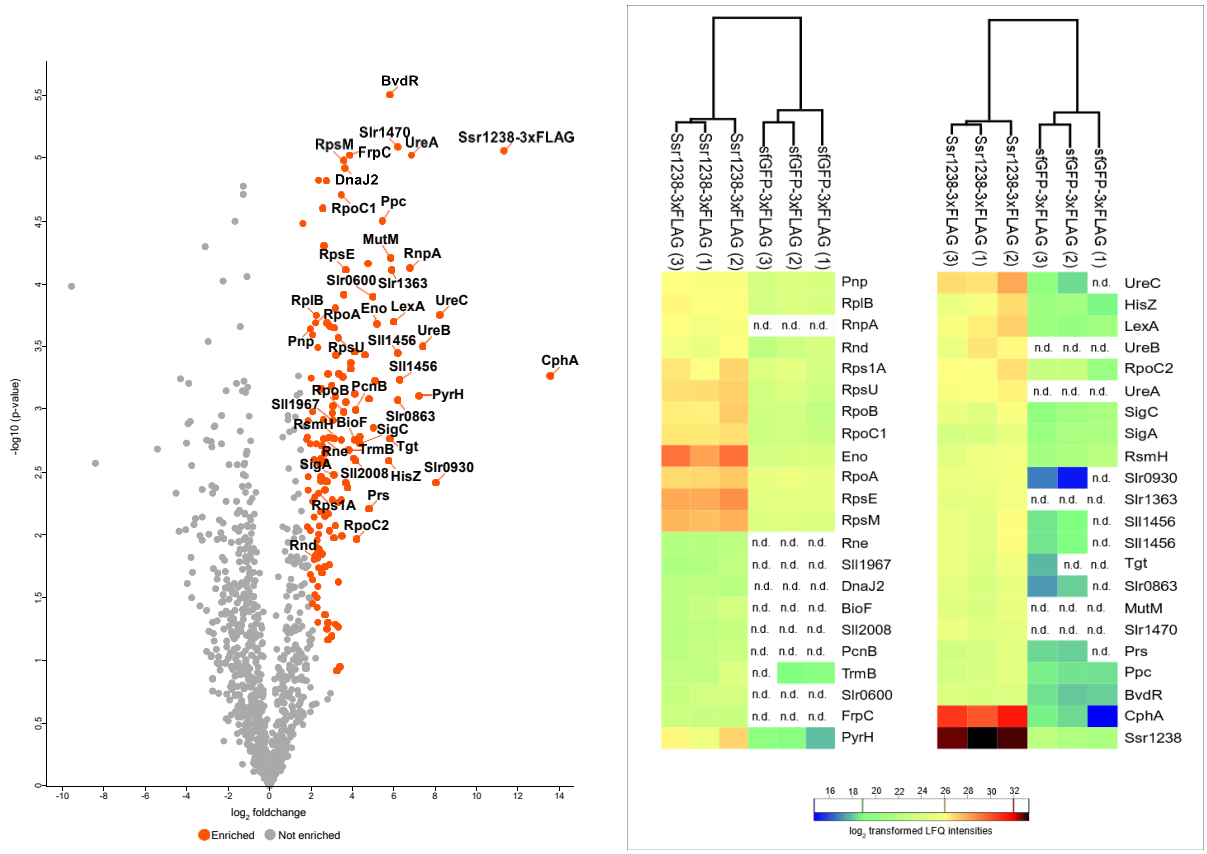

Figure 5. Coimmunoprecipitation experiments for the identification of protein complexes YlxR/Ssr1238 is involved in. A. Volcano plot based on a two-sample t test of enriched proteins using a false discovery rate (FDR) of 0.01 and a coefficient for variance minimization (86) s0 of 2. **B.** Hierarchical clustering of the most abundant proteins detected by mass spectrometry. The two most-enriched proteins are YlxR/Ssr1238 and cyanophycin synthetase (CphA (68)). For the complete list of detected proteins, see **Supplementary Table S6,** for details of the data analyses **Supplementary Tables S7** and **S8**.

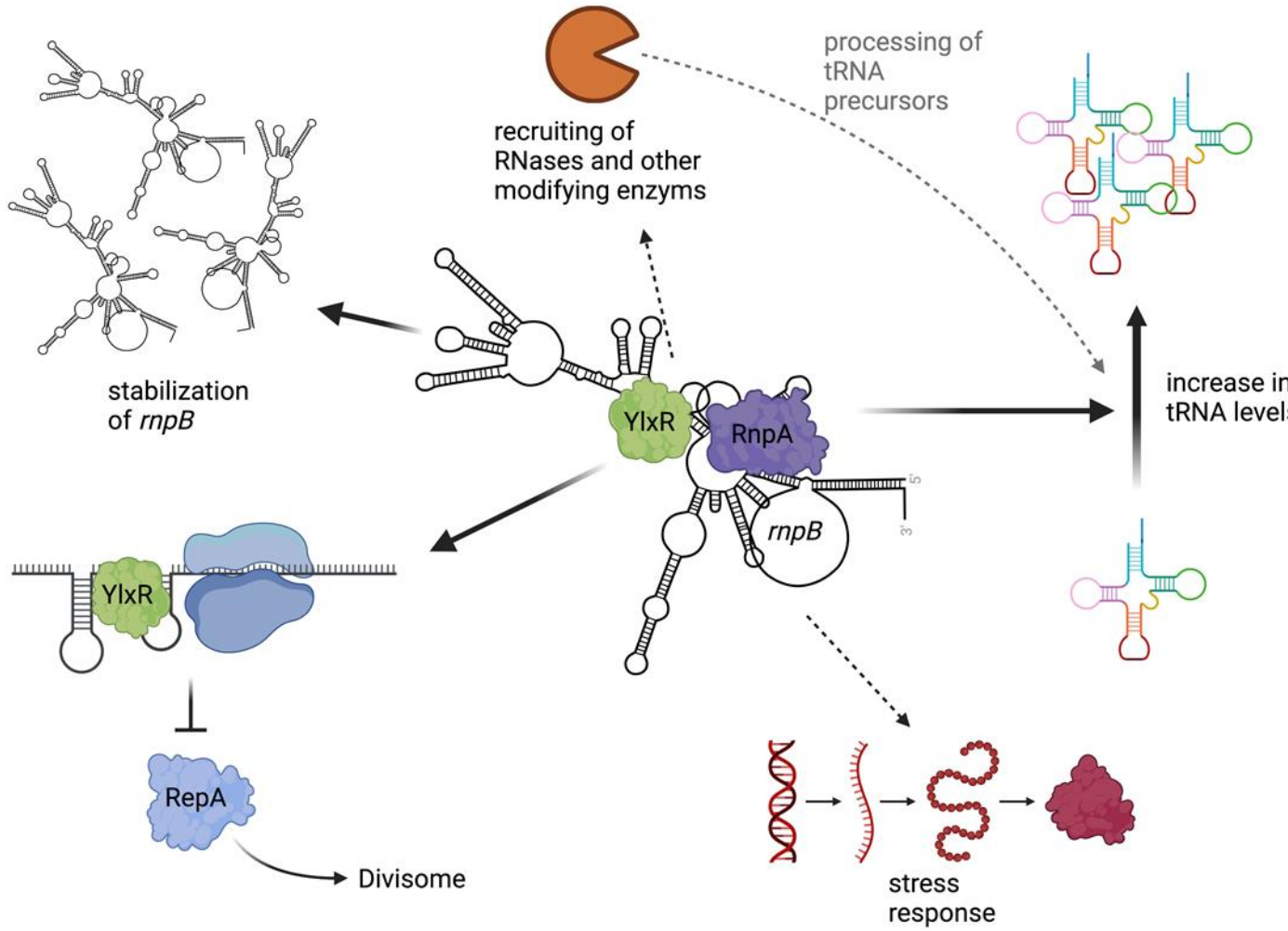

Figure 6. **Proposed model of YlxR/Ssr1238 functions in the context of the cyanobacterial cell.** Middle: YlxR/Ssr1238 binds to RNase P RNA (**Figure 1**), which also interacts with its cognate protein component, RnpA, explaining its high enrichment in the protein interactome (**Figure 5**). Overexpression of YlxR/Ssr1238 also resulted in higher RNase P RNA levels, presumably by stabilizing it (top left corner), and this likely contributed to the slightly elevated tRNA levels observed (**Figure 4**). The protein interactome data also suggested that the RnpA-RnpB-YlxR complex may act in close proximity to ribosomes and interact directly or indirectly, with other key enzymes of RNA metabolism (**Figure 5**). These effects affected the composition of the transcriptome including the upregulation of stress-related mRNAs (lower right corner). Finally, we observed that YlxR/Ssr1238 recruited a stem-loop structure in the rare lipoprotein *repA* mRNA 3' segment (**Figure 3**). This may prevent ribosomes from finishing translation (bottom, left corner). RepA is required for cell division, and once it is produced, it is likely to be recruited to the mid-cell division plane, together with FtsZ.

Whether YlxR switches between the *repA* mRNA and the RNase P RNA or how it dissociates from the *repA* mRNA is a matter for further research. The figure was created with elements from Biorender.com.